

## Original Article

# <sup>18</sup>F-FDG avid volumes on pre-radiotherapy FDG PET as boost target delineation in non-small cell lung cancer

Ang Gao<sup>1\*</sup>, Shijiang Wang<sup>1\*</sup>, Zheng Fu<sup>2</sup>, Xindong Sun<sup>1</sup>, Jinming Yu<sup>1</sup>, Xue Meng<sup>1</sup>

<sup>1</sup>Department of Radiation Oncology, Shandong Cancer Hospital and Institute, Shandong Academy of Medical Sciences, Jinan, China; <sup>2</sup>Department of Nuclear Medicine, Shandong Cancer Hospital and Institute, Jinan, China.  
\*Equal contributors.

Received January 29, 2015; Accepted April 18, 2015; Epub May 15, 2015; Published May 30, 2015

**Abstract:** Background: To investigate whether during/post-radiotherapy FDG uptake locations within tumors is likely identified using a pre-radiotherapy scan for non-small cell lung cancer (NSCLC), ultimately enabling confirm that a suitable metabolically active sub-volume pre-radiotherapy of the primary tumor for radiation boosting target. Methods: Patients with a pathologically proven inoperable stage II-III NSCLC were enrolled. For each patient, one pre-radiotherapy (pre-RT) plus one following 40Gy during-radiotherapy (during-RT) or post-radiotherapy (post-RT) FDG PET/CT scans were available. On pre-RT scan, the high FDG uptake region were auto-delineated using several percentage of the maximal standardized uptake value ( $SUV_{max}$ ) thresholds, varying from 40% to 70%. On during-RT scan, FDG uptake region is delineated by 40%  $SUV_{max}$  manual method respectively. With the FDG-positive areas on post-RT images is defined as 80%  $SUV_{max}$ . The overlap fractions (OFs) were calculated between pre-RT scan and during-RT or post-RT scan. Semi-quantitative assessment was used to determine  $SUV_{max}$  and metabolic tumor volume (MTV). The  $SUV_{max}$  changes during-RT representing the radiotherapy (RT) early metabolic response is attainable. Then, a spearman correlation was used to analysis the correlation between percentage changes in  $SUV_{max}$  during-RT and  $SUV_{max}$ -threshold definition volume pre-RT. Results: Of those 7 patients, a total of 16 FDG-PET scans were acquired. 5 patients were received pre-RT and during-RT scan, while 2 of these 5 patients underwent both post-RT scan. 2 patients were received FDG-PET/CT scan pre-RT and post-RT. The pre-RT scan threshold delineations of 50%  $SUV_{max}$  had a large OF with the 40%  $SUV_{max}$  threshold and manual method delineation on the during-RT scan, 74.3% and 84.4%, respectively. Comparably, the 80%  $SUV_{max}$  on the post-RT scan also largely corresponded (OF > 72%) with the 50%  $SUV_{max}$  threshold and the volume was small compared to the gross tumor volume (GTV), accounting for 29.4%. However, the 50%  $SUV_{max}$  threshold was not correlate with the percentage change in  $SUV_{max}$  (P > 0.05). Conclusions: A pre-RT FDG-PET scan allows for the identification of during- and post-RT FDG uptake locations. The volume defined by 50%  $SUV_{max}$  may be a suitable threshold for dose escalation.

**Keywords:** Non-small cell lung cancer, FDG-PET, SUV-threshold, boost target delineation, dose painting

## Introduction

Currently, patients with inoperable non-small cell lung cancer (NSCLC) are treated with radiation alone for early-stage disease and with chemoradiotherapy (CRT) for locally advanced disease. However, standard radiotherapy (RT) of NSCLC with 60Gy is associated with a 45% to 50% rate of local recurrence [1]. Improvements in local tumor control can be achieved by escalating the radiation dose, but it also increases the incidence and severity of radiation toxicities. Just as the Radiation Therapy Oncology Group (RTOG) 0617 trial [2] showed that the higher radiation dose being tested, 74

Gy could not produce an overall survival benefit compared with the lower, standard dose of 60Gy. One possible explanation is that the survival was affected by the pulmonary or cardio-pulmonary effects of unnecessary irradiation region. Escalated dose to a biological target sub-volumes than GTV defined with current computed tomography (CT)-based imaging, the local tumor control might increase while the current normal tissue complication rates were maintained. Therefore, a strategy to identify a radio-resistance distribution seems necessary.

FDG as a PET tracer for glucose metabolism of tumor, high uptake is associated with a malig-

nant phenotype and poor prognosis [3], and the locations of high FDG uptake zones within the tumor remained stable throughout a fractionated RT course [4]. Therefore, we hypothesized that these high FDG uptake zones before treatment could be the radio-resistance regions. If true, high FDG uptake threshold-based definition of target volumes may increase the efficacy of RT by permitting escalated dose to the regions critical for tumor control.

In fact, a number of centers are exploring the utility of serial PET-CTs to guide dose-escalation, often delivering a boost dose of RT to areas of during RT PET activity [5, 6]. Parallely, some PET-boost trials showed that dose-escalation using threshold-based definition target volumes is feasible with significant increase in prescribed dose without violating the constraints for the organs at risk (OAR) [7, 8]. However, when and where to boost is still uncertain. Therefore, we investigate whether a SUV-threshold metabolically active sub-volume pre-radiotherapy (pre-RT) of the primary tumor is likely the replacement of during/post RT FDG uptake locations. Furthermore, various thresholds definition volume of pre-RT, as well as the correlation between thresholds definition volume of pre-RT and tumor glucose metabolic radio-sensibility index visualized on the middle of RT was investigated to select the optimum cut-off value of high pre-radiotherapy FDG uptake, ultimately enabling selective-boosting of tumor sub-volumes.

## Materials and methods

### *Patient characteristics*

Patients were eligible if they had pathologically proven inoperable stage II or III NSCLC. Other criteria included performance score (PS) 0 to 1, adequate general condition for either RT with or without chemotherapy of curative intent, age > 18 years, and absence of pregnancy. The initial evaluation included a complete history, physical examination with special attention to primary and metastatic lung cancer symptoms, and laboratory tests. Imaging studies including CT of the chest and upper abdomen, and CT or magnetic resonance imaging of the brain with and without contrast.  $^{18}\text{F}$ -FDG PET/CT scan were included as a component of the initial staging, during (at 40 Gy) and/or post the course of therapy.

### *$^{18}\text{F}$ -FDG PET/CT image acquisition*

The FDG-PET/CT scans were performed with a Discovery LS PET/CT scanner (GE Healthcare; Chalfont St. Giles, United Kingdom). Briefly, the patients fasted for at least 6 h before the PET examination and the serum glucose level was measured to ensure the value was less than 6.6 mmol/l. 50-70 minutes after intravenous injection of 10-20 mCi of  $^{18}\text{F}$ -FDG, emission scans were obtained from head to thigh for 4 min per field of view, each covering 14.5 cm, at an axial sampling thickness of 4.25 mm per slice. CT data were collected in helical acquisition mode. No CT contrast agent was administered. The PET and CT scans were obtained during free breathing. PET images were reconstructed with CT-derived attenuation correction using ordered subset expectation maximization (OSEM) software. Pre-RT baseline PET/CT scans were done about 1~3 days before the start of RT. The second whole-body PET/CT scan was recorded at the middle of RT (40 Gy). The post-RT scans were performed at the end of RT.

### *Delineation of CT-based tumor volume and radiotherapy*

The gross tumor volume (GTV) included the primary tumor and involved lymph nodes, and planning target volume included the GTV with a margin of 1.0-1.5 cm. On the basis of axial CT images, contouring of the GTV<sub>CT</sub> for primary tumors in the lung window and metastatic lymph node was performed with the PET result. Contrast uptake helped to differentiate the tumors from the surrounding structures. Lymph nodes were considered pathological when their smallest axis diameter was > 1 cm and/or high FDG uptake was visible. All patients underwent RT, which was delivered with megavoltage equipment (6 MV) using a three-dimensional conformal RT (3D-CRT) technique. Irradiation was given as conventionally fractionated RT with 5×2 Gy per week to a total dose of 60-66 Gy.

### *Image analysis*

Images of the SUV parameter and metabolic tumor volume (MTV) were generated by the use of custom software. Semi-quantitative measurements of metabolic uptake (The SUV<sub>max</sub>) in FDG-avid tumors following pre-RT and during-

**Table 1.** Patients and tumor characteristics

No.	Age (year)	Sex	Pathological type	Tumor stage	Tumor size (cm <sup>3</sup> )*	Nodal stage <sup>#</sup>	clinical stage <sup>#</sup>	SUV <sub>max</sub> of <sup>18</sup> F-FDG uptake		
								Pre-RT	During-RT	Post-RT
1	75	F	SCC	T4	31.45	N0	IIla	24.68	N/A	4.97
2	63	M	SCC	T3	72.42	N2	IIla	21.15	15.48	9.31
3	61	M	AC	T4	161.16	N2	IIlb	11.06	6.12	4.72
4	57	M	AC	T2	18.4	N2	IIla	12.02	N/A	2.77
5	74	M	SCC	T4	95.51	N2	IIlb	17.29	14.2	N/A
6	81	M	SCC	T3	61.34	N0	IIb	29.36	15.8	N/A
7	34	F	SCC	T4	137.63	N1	IIla	15.81	20.75	N/A

Abbreviations: SEX, M male, F female. Pathological type, SCC Squamous cell carcinoma, AC Adenocarcinoma. <sup>18</sup>F-FDG 2-deoxy-2-[<sup>18</sup>F]-fluoro-D-glucose, SUV<sub>max</sub> the maximum standard uptake value, Pre-RT Pre-radiotherapy, During-RT During-radiotherapy, Post-RT Post-radiotherapy. \*Tumor size (cm<sup>3</sup>) was calculated Automatically in Philips workstation when the region of interest delineated. <sup>#</sup>All of the TNM staging information and clinical stage included in this research is according to AJCC Cancer Staging Manual (Seventh Edition).

RT scans were compared and evaluated for radio-sensibility. The percentage change ( $\Delta$ ) in SUV<sub>max</sub> between baseline (pre) and during treatment (during) was calculated using the following formula:

$$\Delta P = \{[P_{\text{pre}} - P_{\text{during}}] / P_{\text{pre}}\} \times 100\%$$

A negative value indicated a reduction in that parameter following therapy and a positive value indicated an increase. The SUV-threshold relative volume of the primary tumor was defined as volume of the various threshold, divided by the volume of GTV pre-RT. Then, the correlation between changes in SUV-threshold definition relative volume and  $\Delta P$  were investigated for testing the relationship between the volume of the different thresholds pre-RT and RT early metabolic response.

On the during-RT and post-RT scan, FDG metabolic areas were accomplished through SUV-threshold definition. On the pre-RT scan, the location and volume of the FDG uptake within the GTV were automatic delineated using the threshold 40, 50, 60 and 70% of SUV<sub>max</sub>. On the during-RT scan, FDG uptake within the GTV were quantified using the threshold 40% of the SUV<sub>max</sub> and manual methods (Manual delineated by an experienced nuclear medicine physician (AES) choosing an appropriate threshold [9]. Within the residual FDG-positive areas post-RT, the high FDG uptake areas were defined using the thresholds 80% of the tumor SUV<sub>max</sub>. Using an automatic rigid registration algorithm based on mutual information of the CT scans, the images of pre-RT scan were fused to the during-RT and post-RT scans on the workstation. If the automatic registration showed a large deformation between the two

CT scans, the images were manually registered on the surrounding anatomy of the tumor, e.g. the bronchus or great vessels. To quantify positional correlation, we calculated the overlap fraction (OF) defined as the overlapping volume of the structure sets, divided by the volume of the smallest structure set [10]:

$$OF = \frac{V_1 \cap V_2}{\min(V_1, V_2)}$$

Where  $V_1$  and  $V_2$  stand for the volumes of the structure sets,  $\cap$  denotes the union, and  $\min(V_1, V_2)$  is the smallest of  $V_1$  and  $V_2$ . The OF was computed for all tumors and thresholds in three dimensions. The OF varied between 0 (no overlap between the structures) and 1 (complete overlap of one structure with the other) [4]. By using this methodology it is possible to assess which threshold on the pre-RT scan matches the disease on the during-RT and post-RT scan.

### Statistical analysis

Data are expressed as mean  $\pm$  standard deviation (SD) and range. Statistical significant differences between the parameters were performed using commercial software SPSS for Windows (version 17.0). A Spearman rank correlation analysis was used to estimate the correlation between the percentage change in SUV<sub>max</sub> ( $\Delta P$ ) and the MTV delineated using various threshold on the pre-RT scan,  $P < 0.05$  was considered significant.

## Result

### Patient characteristics

The patients' characteristics are presented in **Table 1**. A total of 7 patients were included in

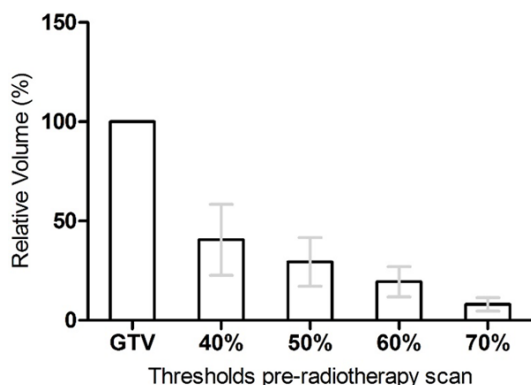


**Figure 1.** Volumes of the SUV thresholds of the tumor pre-radiotherapy. All volumes are relative to the pre-radiotherapy gross tumor volume (GTV). The data are expressed as mean  $\pm$  standard deviation (error bar). Note that the volume of 50%  $SUV_{max}$  thresholds metabolic-active areas was on average 29% of GTV volume.

our study. Four treated with two cycles of concurrent conformal radiation therapy with a cisplatin-based regimen. One with sequential CRT and two with radical RT alone. A total of 16 FDG-PET scans were acquired. Two FDG-PET/CT scan were available for five patients: three patients were received FDG-PET/CT scan were included as a component of the initial staging and during the course of therapy, two patients were received FDG-PET/CT scan before start of RT and after the end of RT, while another two patients underwent three FDG-PET scan, one pre-RT, one during-RT and one at the end of RT. All of these patients had a clearly distinguishable lesion from the surrounding tissue and FDG avid inflammation.

#### Volumes of the SUV based thresholds

The volumes of the SUV based thresholds of the tumor pre-RT are shown in **Figure 1**. The volume of interest (VOI) on pre-RT scan was compared with manually delineated GTV of primary tumor defined on CT scan. The FDG uptake areas (40-70%  $SUV_{max}$ ) within the tumor on the pre-RT scan were small compared to the GTV. The 40%  $SUV_{max}$  encompassed  $40.5 \pm 17.9\%$  [range: 17.9-71.75%] of the original GTV. A very large proportion (71.75%) of primary tumor was contained in No.3 patients. Whereas this was  $29.4 \pm 12.3\%$  [range: 11.3-49.7%] for the 50%  $SUV_{max}$ ,  $19.4 \pm 7.6\%$  [range: 6.8-30.0%] for the 60%  $SUV_{max}$ , and  $8.1 \pm 3.4\%$  [range: 4.3-13.3%] for the 70%  $SUV_{max}$  threshold. No signifi-

cant difference was found among the relative volumes of 40-70%  $SUV_{max}$  thresholds. The limited OFs applying the 70% threshold resulted from the low volumes of the threshold on pre-RT scan [ $7.5 \pm 6.4 \text{ cm}^3$ ; range: 1.2-18.2  $\text{cm}^3$ ], often only a few image voxels.

#### Overlap fractions

We correlated volumes of FDG uptake measured during- and/or post-RT with that of pre-RT (40-70%  $SUV_{max}$ ) by calculating the overlap fraction, given by Eq [10]. In **Figure 2**, representative images are shown. The high FDG uptake areas (50%  $SUV_{max}$ ) on the pre-RT scan overlapped the location of during and post-RT areas are shown in one patient. In the undergoing pre-RT plus during-RT population, the 40% thresholds showed large overlap with during-RT for auto-delineation method ( $78.3 \pm 15.3\%$ ). Moreover, the same is true for pre-RT 50%  $SUV_{max}$  high FDG uptake region ( $74.3 \pm 15.9\%$ ). However, the 60% and 70% thresholds showed relative low overlap fractions,  $68.1 \pm 18.0\%$ ,  $64.2 \pm 24.2\%$ , respectively. Significant difference was found between the 50% and 60% thresholds ( $P < 0.05$ ). The pre-RT 50%  $SUV_{max}$  threshold areas also largely corresponded with post-RT residual areas (80%  $SUV_{max}$  threshold), to show the overlap fraction were  $72.4 \pm 23.7\%$ . But there was no significant difference among 40%-70% thresholds. It is worth nothing that all of the OF were up to  $87.1 \pm 12.8\%$ ,  $84.4 \pm 15.3\%$ ,  $79.8 \pm 22.4\%$ ,  $76.3 \pm 34.9\%$ , for manual method as shown in **Figure 3A**. But again no significant difference was found. Visual evaluation shows that the location of during- and post-RT areas largely corresponds with the high FDG uptake areas (50%  $SUV_{max}$ ) pre-RT, especially for the during-RT delineated by manual method.

#### Correlation between $SUV_{max}$ changes during RT and threshold relative volume

Undergoing pre-RT plus during-RT  $^{18}\text{F}$ -FDG PET scans were available for 5 patients. The  $SUV_{max}$  of all the primary tumor decreased in the mid-treatment scan except one ( $SUV_{max}$  was 15.81 raise to 20.75 and  $SUV_{mean}$  was 7.77 raise to 7.96). The  $SUV_{max}$  and  $SUV_{mean}$  inside the PET volume was  $18.9 \pm 6.9$  and  $9.7 \pm 5.7$ , respectively, for the pretreatment scan, compared with  $14.5 \pm 5.3$  and  $7.9 \pm 3.2$  (40% threshold),  $6.1 \pm 1.8$  (manual delineation) respectively, for



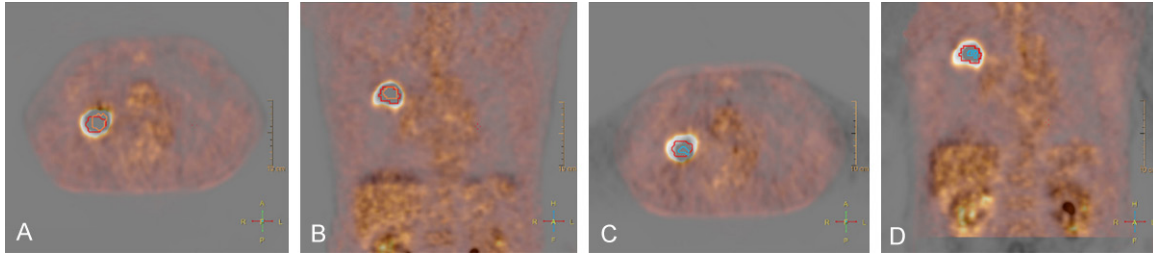


**Figure 2.** Representative FDG-PET CT fused images of a patient pre-plus during-RT (A, B) and post-RT (C, D). The red lines indicate the 50% of maximal standardized uptake value ( $SUV_{max}$ ) threshold pre-radiotherapy. The yellow lines indicate the 40%  $SUV_{max}$  threshold during-radiotherapy and the blue lines indicate the 80%  $SUV_{max}$  threshold post-radiotherapy, transposed on the pre-radiotherapy scan. Visual inspection showed a large correspondence between the FDG high uptake areas during-radiotherapy and post-radiotherapy with the high FDG uptake areas pre-radiotherapy.

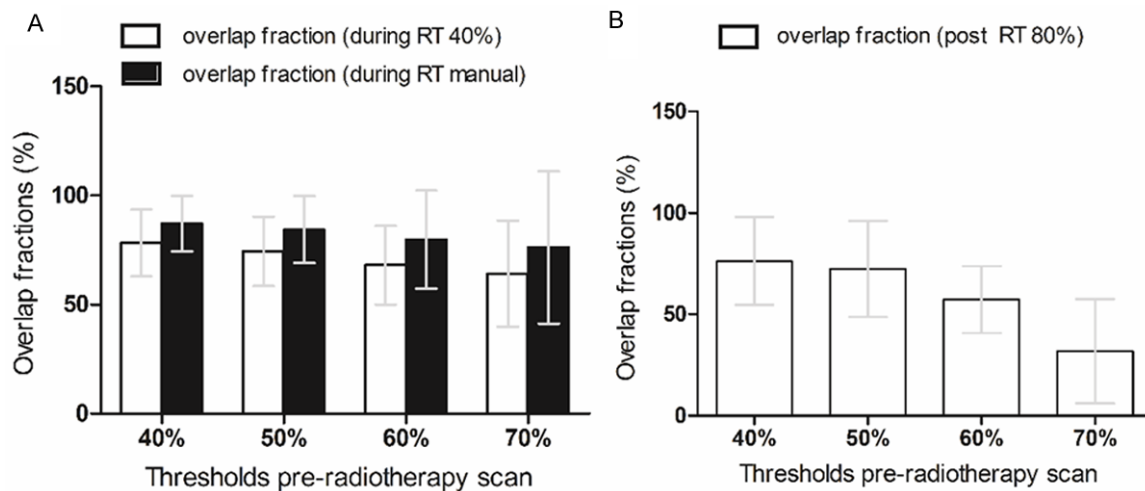


**Figure 3.** Overlap fractions (OFs) of the pre-radiotherapy with the during-radiotherapy (A) and post-radiotherapy (B)  $SUV_{max}$  thresholds. OFs of the FDG-uptake (40% thresholds and manual method) areas during-RT are indicated with white and black-bars (A). In (B), white-bars indicate the OF of 80%  $SUV_{max}$  post-RT. The data are expressed as mean  $\pm$  standard deviation (error-bars). The 40% and 50% thresholds Pre-RT showed high overlap fractions with  $^{18}F$ -FDG-uptake during-RT and post-RT.

the mid-treatment scan. The percentage change ( $\Delta$ ) (between pre and during) in  $SUV_{max}$  and the 70%  $SUV_{max}$  relative volume within the tumor on the pre-RT scan were significantly correlation. ( $r = -0.8$ ,  $P < 0.05$ ). This would imply that a responder during-RT will be implemented a smaller boosting region. However, the 40%, 50%, 60%  $SUV_{max}$  threshold were not correlate with the percentage change ( $\Delta$ ) in  $SUV_{max}$  ( $P > 0.05$ ).

### Discussion

High-dose radiation has the potential to improve local-regional control and overall survival after fractionated therapy. However, it is challenging to deliver a high dose in the majority of patients with locally advanced NSCLC. To

explore the utility of pre-RT  $^{18}F$ -FDG PET for guiding biologically optimized boosting target, we compared sub-volumes defined with different levels of FDG uptake quantified with  $SUV_{max}$  of the pre-radiotherapy and subsequent during- or post-radiotherapy  $^{18}F$ -FDG PET of primary tumors. The study proved that the location of residual metabolic-active areas within the primary tumor during and post-RT corresponded with the original high FDG uptake areas pre-radiotherapy, and 50%  $SUV_{max}$  threshold intensity value identified as a reasonable value. Irradiating only 50%  $SUV_{max}$  threshold regions may allow dose escalation by treating smaller volumes.

Individual treatment is a goal in modern cancer therapy, with the aim that optimal dose-escala-

tion area can be selected for an individual patient depending on tumor characteristics. Based on the previous studies that tumor response is heterogeneous during chemo/RT and tumor volume reduced ~20% more on PET than on CT, a randomized Phase II Trial RTOG 1106 is ongoing to determine whether PET during-RT (at 40-46 Gy) can guide individualized, adaptive RT to deliver a more intensive dose to the active residual tumor resulting in improved local tumor control. Interestingly, manual delineation method during-RT overlapped with FDG-uptake based various thresholds on pre-RT yields relative better results in our result. Especially 40%  $SUV_{max}$  resulting in an overlap fraction of 87%. This finding suggest that metabolic active areas within the tumor during-RT can be predicted using an high FDG uptake area on pre-RT scan, and 40%  $SUV_{max}$  maybe a suitable threshold. Therefore, we inferred that FDG high uptake pre-RT might reminder individualized information in boosting targets as RTOG 1106 performed.

In the present study, we demonstrated that the during- and post-RT high uptake areas correspond with these contours areas pre-RT. The 40%  $SUV_{max}$  and 50%  $SUV_{max}$  zones have a good overlap fraction, but the 40%  $SUV_{max}$  areas approximate the cut-off value for target volume [11, 12], therefore, nearly entire primary tumor dose-escalation will be implement in some case (e.g., diameter at CT imaging < 3 cm or pathologic volume for 10-30 cm<sup>3</sup> tumors) [13]. In especial, large tumor volumes lead to irradiation of a larger volume of the lung and hence, constraints on dose to the lung will limit dose escalation. Using 50%  $SUV_{max}$  threshold value will make dose escalation to higher dose levels available to a broader range of patients on account of the good OF and volume ratio. It makes the 50%  $SUV_{max}$  threshold value a suitable threshold for radiation boosting target. Disappointingly, the volume of 50%  $SUV_{max}$  delineated was not correlation with radio-sensitivity index in present study. The 60%  $SUV_{max}$  threshold was encompassed  $19.4 \pm 7.6\%$  [range: 6.8-30.0%] of the original GTV and its relative low OF, the risk of local recurrences on the periphery of the planning target volume was increased. The study was presented that only 70%  $SUV_{max}$  zones showed significantly correlation with radio-sensitivity index. Yet, 70%  $SUV_{max}$  areas would lead to only a few voxels to be

treated, which is often impossible due to organ motion or dose delivery constraints.

Indeed, cellular hypoxia is known to be directly related with radio-resistance. However, several nitroimidazole for PET hypoxia imaging (like FMISO, FAZA, EF-3, and EF-5) have limitations, essential questions is low test re-test performance and the reproducibility of the intratumoral distribution of hypoxia [14, 15]. There is a lot of uncertainty about how specific these traces relate to radio-resistance [15, 16]. Furthermore, it is unknown if areas with high trace uptake have the highest probability to relapse. Due to these reasons, more evidence is desirable to use hypoxia tracers PET only for dose intensification [17].

Based on our results, we conclude that during- and post-RT high uptake areas within the tumor can be identified before treatment using an FDG PET/CT scan, affirming the relation between FDG uptake and radio-resistance. But a previous study by Nyflot showed that voxel-based correlation of FDG PET and Cu-ATSM PET images were heterogeneity ( $r = 0.64$ ) in oropharynx cancer [18]. According to our view, excepting for the uncertainty of PET hypoxia imaging, one possible explanation is that heterogeneity in tumor phenotype indicated poor patient prognosis. Another potential possibility is that the FDG volume may be missing hypoxic subregions. In fact, the FDG uptake in the tumor does not reflect a single biologic characteristic [19], but is correlated to, although certainly not specific for many pathways that are related to radio-resistance, such as cell density, mitochondrial dysfunction, hypoxia, proliferation and lipogenesis. This is likely the reason why 50%  $SUV_{max}$  not correlation with radio-sensitivity index. In our view, to cap the certainty about the radio-resistance of tumor anywhere in the target region, the combination of multiple Functional imaging modalities (FI) can increase sensitivity and specificity [20], but leaves the question how multiple FI can be harnessed for identifying the radiation resistance area [21].

A limitation of our study is the registration between the pre- and during- or post-scans. The lung tumors were sensitivity to breathing motion [22, 23], gating techniques during the acquisition of the PET/CT would have further reduced the sensitivity to respiratory motion [24, 25]. Otherwise, the wide time range, par-

ticularly for tumors was just post-treatment, can be complicated by changes in various factor making the registration sophisticated. This could be improved by using deformable image registration [26]. However, these are difficult to validate and the reproducibility, especially in different institutes, is limited. Finally, a rigid registration based on the anatomical structure around the tumor was performed in our study.

## Conclusion

Our results were validated that the residual metabolic-active areas within the tumor during- and post-radiotherapy are located in the high uptake areas pre-radiotherapy can be delineated and the 50%  $SUV_{max}$  threshold value delineation using automatic image segmentation tools may be a suitable threshold for dose escalation. However, the combination of multiple functional imaging modalities to guide boost target delineation is needed to investigate in further study.

## Acknowledgements

This work was supported by the National Natural Science Foundation of China (8147-2810), the encouraging fund of scientific research for excellent young and middle-aged scientist of Shandong province (BS2011YY015) and Science Foundation of China post-doctor (2013M531608).

## Disclosure of conflict of interest

None.

**Address correspondence to:** Dr. Xue Meng, Department of Radiation Oncology, Shandong Cancer Hospital and Institute, Shandong Academy of Medical Sciences, Jiyuan Road 440, Jinan, China. Tel: 86-531-67626142; Fax: 86-531-67626141; E-mail: mengxue5409@126.com

## References

- [1] Machtay M, Bae K, Movsas B, Paulus R, Gore EM, Komaki R, Albain K, Sause WT and Curran WJ. Higher biologically effective dose of radiotherapy is associated with improved outcomes for locally advanced non-small cell lung carcinoma treated with chemoradiation: an analysis of the Radiation Therapy Oncology Group. *Int J Radiat Oncol Biol Phys* 2012; 82: 425-434.
- [2] Bradley JD, Paulus R, Komaki R, Masters G, Blumenschein G, Schild S, Bogart J, Hu C, Forster K, Magliocco A, Kavadi V, Garces YI, Narayan S, Iyengar P, Robinson C, Wynn RB, Koprowski C, Meng J, Beitler J, Gaur R, Curran W Jr and Choy H. Standard-dose versus high-dose conformal radiotherapy with concurrent and consolidation carboplatin plus paclitaxel with or without cetuximab for patients with stage IIIA or IIIB non-small-cell lung cancer (RTOG 0617): a randomised, two-by-two factorial phase 3 study. *Lancet Oncol* 2015; 16: 187-99.
- [3] Allal AS, Slosman DO, Kebdani T, Allaoua M, Lehmann W and Dulguerov P. Prediction of outcome in head-and-neck cancer patients using the standardized uptake value of 2-[18F] fluoro-2-deoxy-D-glucose. *Int J Radiat Oncol Biol Phys* 2004; 59: 1295-1300.
- [4] Aerts HJ, Bosmans G, van Baardwijk AA, Dekker AL, Oellers MC, Lambin P and De Ruyscher D. Stability of 18F-deoxyglucose uptake locations within tumor during radiotherapy for NSCLC: a prospective study. *Int J Radiat Oncol Biol Phys* 2008; 71: 1402-1407.
- [5] Feng M, Kong FM, Gross M, Fernando S, Hayman JA and Ten Haken RK. Using fluorodeoxyglucose positron emission tomography to assess tumor volume during radiotherapy for non-small-cell lung cancer and its potential impact on adaptive dose escalation and normal tissue sparing. *Int J Radiat Oncol Biol Phys* 2009; 73: 1228-1234.
- [6] Gillham C, Zips D, Ponisch F, Evers C, Enghardt W, Abolmaali N, Zophel K, Appold S, Holscher T, Steinbach J, Kotzerke J, Herrmann T and Baumann M. Additional PET/CT in week 5-6 of radiotherapy for patients with stage III non-small cell lung cancer as a means of dose escalation planning? *Radiother Oncol* 2008; 88: 335-341.
- [7] van Elmpt W, De Ruyscher D, van der Salm A, Lakeman A, van der Stoep J, Emans D, Damen E, Ollers M, Sonke JJ and Belderbos J. The PET-boost randomised phase II dose-escalation trial in non-small cell lung cancer. *Radiother Oncol* 2012; 104: 67-71.
- [8] Moller DS, Khalil AA, Knap MM, Muren LP and Hoffmann L. A planning study of radiotherapy dose escalation of PET-active tumour volumes in non-small cell lung cancer patients. *Acta Oncol* 2011; 50: 883-888.
- [9] Edet-Sanson A, Dubray B, Doyeux K, Back A, Hapdey S, Modzelewski R, Bohn P, Gardin I and Vera P. Serial assessment of FDG-PET FDG uptake and functional volume during radiotherapy (RT) in patients with non-small cell lung cancer (NSCLC). *Radiother Oncol* 2012; 102: 251-257.

- [10] Siegel R, Ma J, Zou Z and Jemal A. Cancer statistics, 2014. *CA Cancer J Clin* 2014; 64: 9-29.
- [11] Erdi YE, Mawlawi O, Larson SM, Imbriaco M, Yeung H, Finn R and Humm JL. Segmentation of lung lesion volume by adaptive positron emission tomography image thresholding. *Cancer* 1997; 80: 2505-2509.
- [12] Black QC, Grills IS, Kestin LL, Wong CY, Wong JW, Martinez AA and Yan D. Defining a radiotherapy target with positron emission tomography. *Int J Radiat Oncol Biol Phys* 2004; 60: 1272-1282.
- [13] Yu J, Li X, Xing L, Mu D, Fu Z, Sun X, Sun X, Yang G, Zhang B, Sun X and Ling CC. Comparison of tumor volumes as determined by pathologic examination and FDG-PET/CT images of non-small-cell lung cancer: a pilot study. *Int J Radiat Oncol Biol Phys* 2009; 75: 1468-1474.
- [14] Dubois L, Landuyt W, Cloetens L, Bol A, Bormans G, Haustermans K, Labar D, Nuyts J, Gregoire V and Mortelmans L. [18F]EF3 is not superior to [18F]FMISO for PET-based hypoxia evaluation as measured in a rat rhabdomyosarcoma tumour model. *Eur J Nucl Med Mol Imaging* 2009; 36: 209-218.
- [15] Nehmeh SA, Lee NY, Schroder H, Squire O, Zanzonico PB, Erdi YE, Greco C, Mageras G, Pham HS, Larson SM, Ling CC and Humm JL. Reproducibility of intratumor distribution of (18)F-fluoromisonidazole in head and neck cancer. *Int J Radiat Oncol Biol Phys* 2008; 70: 235-242.
- [16] Maftei CA, Shi K, Bayer C, Astner ST and Vaupel P. Comparison of (immuno-)fluorescence data with serial [(1)(8)F]Fmiso PET/CT imaging for assessment of chronic and acute hypoxia in head and neck cancers. *Radiother Oncol* 2011; 99: 412-417.
- [17] Aerts HJ, Lambin P and Ruyscher DD. FDG for dose painting: a rational choice. *Radiother Oncol* 2010; 97: 163-164.
- [18] Nyflot MJ, Harari PM, Yip S, Perlman SB and Jeraj R. Correlation of PET images of metabolism, proliferation and hypoxia to characterize tumor phenotype in patients with cancer of the oropharynx. *Radiother Oncol* 2012; 105: 36-40.
- [19] van Baardwijk A, Dooms C, van Suylen RJ, Verbeken E, Hochstenbag M, Dehing-Oberije C, Rupa D, Pastorekova S, Stroobants S, Buell U, Lambin P, Vansteenkiste J and De Ruyscher D. The maximum uptake of (18)F-deoxyglucose on positron emission tomography scan correlates with survival, hypoxia inducible factor-1alpha and GLUT-1 in non-small cell lung cancer. *Eur J Cancer* 2007; 43: 1392-1398.
- [20] Van den Bergh L, Isebaert S, Koole M, Oyen R, Joniau S, Lerut E, Deroose CM, De Keyser F, Van Poppel H and Haustermans K. Does 11C-choline PET-CT contribute to multiparametric MRI for prostate cancer localisation? *Strahlenther Onkol* 2013; 189: 789-795.
- [21] Alber M and Thorwarth D. Multi-modality functional image guided dose escalation in the presence of uncertainties. *Radiother Oncol* 2014; 111: 354-359.
- [22] Bissonnette JP, Franks KN, Purdie TG, Moseley DJ, Sonke JJ, Jaffray DA, Dawson LA and Bezjak A. Quantifying interfraction and intrafraction tumor motion in lung stereotactic body radiotherapy using respiration-correlated cone beam computed tomography. *Int J Radiat Oncol Biol Phys* 2009; 75: 688-695.
- [23] Thomas JG, Kashani R, Balter JM, Tatro D, Kong FM and Pan CC. Intra and interfraction mediastinal nodal region motion: implications for internal target volume expansions. *Med Dosim* 2009; 34: 133-139.
- [24] Tahari AK, Lodge MA and Wahl RL. Respiratory-gated PET/CT versus delayed images for the quantitative evaluation of lower pulmonary and hepatic lesions. *J Med Imaging Radiat Oncol* 2014; 58: 277-282.
- [25] Knudtsen IS, Rodal J, Brustugun OT, Helland A, Skretting A and Malinen E. Dynamic respiratory gated (18)FDG-PET of lung tumors - a feasibility study. *Acta Oncol* 2011; 50: 889-896.
- [26] Zhang J, Chen L, Wang X, Teng Z, Brown AJ, Gillard JH, Guan Q and Chen S. Compounding local invariant features and global deformable geometry for medical image registration. *PLoS One* 2014; 9: e105815.